P2Y$_{12}$ regulates platelet adhesion/activation, thrombus growth, and thrombus stability in injured arteries

Patrick André,[1] Suzanne M. Delaney,[1] Thomas LaRocca,[1] Diana Vincent,[1] Francis DeGuzman,[1] Marzena Jurek,[1] Beverley Koller,[2] David R. Phillips,[1] and Pamela B. Conley[1]

[1]Cardiovascular Biology, Millennium Pharmaceuticals Inc., South San Francisco, California, USA
[2]Department of Medicine, University of North Carolina, Chapel Hill, North Carolina, USA

The critical role for ADP in arterial thrombogenesis was established by the clinical success of P2Y$_{12}$ antagonists, currently used at doses that block 40–50% of the P2Y$_{12}$ on platelets. This study was designed to determine the role of P2Y$_{12}$ in platelet thrombosis and how its complete absence affects the thrombotic process. P2Y$_{12}$-null mice were generated by a gene-targeting strategy. Using an in vivo mesenteric artery injury model and real-time continuous analysis of the thrombotic process, we observed that the time for appearance of first thrombus was delayed and that only small, unstable thrombi formed in *P2Y$_{12}$$^{-/-}$* mice without reaching occlusive size, in the absence of aspirin. Platelet adhesion to vWF was impaired in *P2Y$_{12}$$^{-/-}$* platelets. While adhesion to fibrinogen and collagen appeared normal, the platelets in thrombi from *P2Y$_{12}$$^{-/-}$* mice on collagen were less dense and less activated than their WT counterparts. *P2Y$_{12}$$^{-/-}$* platelet activation was also reduced in response to ADP or a PAR-4–activating peptide. Thus, *P2Y$_{12}$* is involved in several key steps of thrombosis: platelet adhesion/activation, thrombus growth, and stability. The data suggest that more aggressive strategies of *P2Y$_{12}$* antagonism will be antithrombotic without the requirement of aspirin cotherapy and may provide benefits even to the aspirin-nonresponder population.

Introduction

Platelets are critical mediators of primary hemostasis through adhesion, aggregation, and subsequent thrombus formation induced by collagen, vWF, thrombin, and other factors exposed at sites of vascular injury. This function of platelets can become pathological in atherosclerotic arteries, causing vascular occlusions resulting in stroke or myocardial infarction. Two antiplatelet strategies have proven to be successful for the prevention of major arterial thrombosis. One strategy targets the glycoprotein IIb-IIIa (GP IIb-IIIa) complex (tirofiban, abciximab, eptifibatide), the platelet GP receptor mediating platelet aggregation. The clinical benefit of GP IIb-IIIa antagonists in acute settings is mediated by inhibition of both vWF- and fibrinogen–GP IIb-IIIa interactions, thereby preventing thrombus growth and stability, respectively (1). The other strategy uses thienopyridine drugs (e.g., ticlopidine or clopidogrel) to target the recently identified ADP receptor (P2Y$_{12}$) (2). P2Y$_{12}$ is the G$_{\alpha i}$-coupled receptor mediating inhibition of adenylyl cyclase and is essential for stabilization of platelet aggregates. This receptor has been shown to be defective in a patient with a mild bleeding disorder and abnormal ADP-induced aggregation (2). A second ADP receptor, P2Y$_1$, has also been identified. This receptor couples to G$_{\alpha q}$ and is responsible for mediating platelet shape change and ADP-induced aggregation by mobilization of intracellular calcium (3).

Although it is readily apparent why GP IIb-IIIa antagonists inhibit thrombosis, it is less apparent why P2Y$_{12}$ antagonists provide a therapeutic benefit. First, ADP is considered a weak platelet agonist. Second, ticlopidine and clopidogrel are used at doses that block ADP-mediated ex vivo aggregation by only 40–50% (4), and although they showed clinical benefit alone (5), they are more efficacious when used in combination with aspirin (ASA) (6). Other studies, however, have established that ADP is involved in multiple steps of platelet thrombosis. Firstly, ADP is released from dense granules upon platelet activation: the secreted ADP constitutes a positive-feedback loop in the setting of platelet aggregation independent of the agonist used (7, 8) and contributes to the recruitment of platelets to a growing thrombus as evidenced by the effect of soluble ecto-ADPase/CD39 in vitro (9) and in vivo (10). Secondly, P2Y$_{12}$ and its cognate G$_i$-coupled protein (Gi$_{\alpha 2}$) are probably directly involved in the signaling events generated by other platelet receptors such as GP VI (11) and GP Ibα (12).

This suggests a direct role for P2Y$_{12}$ not only in thrombus stabilization but also in the recruitment of circulating platelets onto a thrombogenic surface (vessel wall injury and adhering platelets).

This study was designed to determine the role of P2Y$_{12}$ in platelet thrombosis and to determine how the complete absence of this ADP receptor affects the thrombotic process. Using P2Y$_{12}$-deficient mice, our in vivo and ex vivo studies show that P2Y$_{12}$ is involved in thrombus growth and stability and that these activities are mediated by mechanisms involving both platelet adhesion and activation. We also find that the total deficiency of P2Y$_{12}$ markedly impacts in vivo thrombosis, even in the absence of ASA.

Methods

Generation of P2Y$_{12}^{-/-}$ mice. The *P2Y$_{12}$* targeting vector was prepared from genomic clones containing the mouse *P2Y$_{12}$* gene. A bacterial artificial chromosome (BAC) clone containing the murine *P2Y$_{12}$* (m*P2Y$_{12}$*) sequence was amplified by PCR screening of a mouse 129/Sv library (Incyte Genomics Inc., St. Louis, Missouri, USA) using primers derived from the coding sequence of m*P2Y$_{12}$*. A 15-kb HindIII fragment was identified from the mouse BAC clone, which contained the m*P2Y$_{12}$* locus. Using PCR primers, a 5′ HindIII site and a 3′ Xba site were introduced to generate a 4-kb fragment just upstream of the ATG initiation codon for mP2Y$_{12}$. Similarly, a XhoI site and NotI site were introduced by PCR to generate a 6-kb 3′ arm. Both of these fragments were subcloned into the pLNL vector such that they flanked a neomycin resistance gene (neo) (Figure 1a). The vector was linearized with PvuI and introduced into the ES cell line E14Tg2a (derived from 129/Ola) by electroporation, and neomycin-resistant clones were selected in media containing G418. DNA was isolated from surviving colonies, digested with XbaI, and assessed by Southern blot analysis using a probe corresponding to a DNA sequence located downstream of the targeting construct. Chimeric mice were generated with P2Y$_{12}$-targeted ES cell lines and were bred to C57BL/6 mice. Mice with the targeted mutation were identified by Southern blot analysis or PCR and intercrossed with siblings that inherited the WT 129 P2Y$_{12}$ allele. Control and experimental mice were then obtained by intercross of the heterozygous mice derived from those sibling intercrosses.

Hemostatic parameters. Aggregation using platelet-rich plasma (PRP) was measured turbidimetrically using a Chronolog aggregation analyzer (Chronolog Corp., Havertown, Pennsylvania, USA) following calibration with platelet-poor plasma, at a stirring speed of 800 rpm. Aliquots (250 μl) of PRP were placed in cuvettes containing magnetic stirrer bars, warmed at 37°C, and stirred for 1 minute to obtain a stable baseline. Aggregation was induced by either ADP (0.5 or 10 μM), collagen (1 or 20 μg/ml), or murine TRAP (mTRAP) (AYPGKF; 1 or 2.5 mM), and change in light transmittance was recorded for 6 minutes. Inhibition of cyclooxygenase by ASA was confirmed by obtaining mouse PRP 2 hours after ASA treatment and measuring aggregation induced by 500 μM arachidonic acid (Cayman Chemical Inc., Ann Arbor, Michigan, USA).

Mice used for bleeding time were sex-matched littermates of heterozygous breeding pairs of a mixed 129/Sv and C57BL/6J background. Genotyping was performed after the bleeding time study by an investigator blinded to the experiment. Male and female progeny (10–13 weeks) were anesthetized (by subcutaneous injection) with ketamine cocktail (ketamine [75 mg/kg; Fort Dodge Animal Health, Fort Dodge, Iowa, USA)], xylazine [8 mg/kg; Vetus, Burns Veterinary Supply Inc., Westbury, New York, USA], and acepromazine [1.5 mg/kg; Vetus]) 6 minutes prior to tail transection. Mice were laid in lateral recumbency on a firm surface with the tail straight out. Tails were transected 2 mm from the tip with a number 10 scalpel blade (Bard-Parker; Becton Dickinson, Franklin Lakes, New Jersey, USA) and immediately immersed into a 20-ml scintillation vial filled with normal saline held at 37°C. A stopwatch was started immediately upon transection to determine time to cessation of bleeding or 15 minutes, whichever occurred first. If bleeding
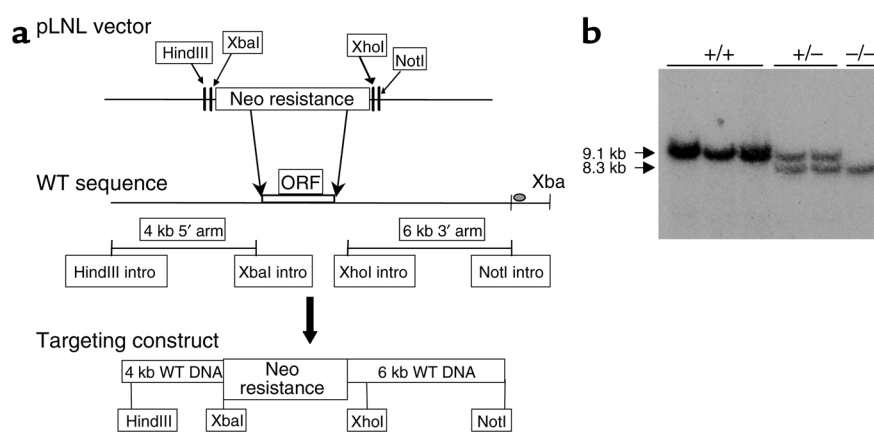

Figure 1

Targeting the *P2Y$_{12}$* locus. (**a**) The neomycin resistance gene in pLNL is flanked by a 4-kb (5′) and 6-kb (3′) fragment from the *P2Y$_{12}$* genomic locus. HindIII, XbaI, XhoI, and NotI sites were introduced by PCR. The WT *P2Y$_{12}$* coding exon is denoted as ORF. ORF, open reading frame.(**b**) Southern hybridizations of XbaI-digested mouse genomic DNA from progeny of breeding pairs heterozygous at the mutant allele. The XbaI fragment detected by the indicated probe (gray oval in Figure 1a) is reduced from 9.1 to 8.3 kb due to introduction of a new XbaI site in the targeted locus. Intro, introduction.

did not reoccur within 60 seconds of cessation, bleeding was considered stopped.

Determination of cAMP. Platelet cAMP levels were measured using the cAMP-Screen ELISA System (Perkin-Elmer Applied Biosystems, Foster City, California, USA). Following incubation with 500 μM 3-isobutyl-1-methylxanthine (Sigma-Aldrich, St. Louis, Missouri, USA) for 10 minutes at 37°C, mouse washed platelets (2.5×10^8/ml, prepared as previously described) (13) were treated with 10 μM ADP (Sigma-Aldrich) or 0.001, 0.1, or 10 μM epinephrine (Burns Veterinary Supply, Farmers Branch, Texas, USA) in the presence of 50 μM forskolin (Sigma-Aldrich) for 10 minutes. Reactions were terminated, processed, and quantitated according to manufacturer's instructions.

Intravital microscopy. Blood sampling and platelet preparation were performed as described previously with minor modifications (14). Blood (approximately 800 μl per mouse) was collected in polypropylene tubes containing 140 μl of acid-citrate-dextrose (38 mM citric acid, 75 mM trisodium citrate, and 100 mM dextrose), 400 μl of washing buffer (129 mM NaCl, 13.6 mM trisodium citrate, 11.1 mM dextrose, 1.6 mM KH$_2$PO$_4$, 0.02 U/ml apyrase, pH 6.8), and 1 μM PGE$_1$ (Sigma-Aldrich). PRP was obtained by centrifugation at 220 *g* for 7 minutes. The plasma and buffy coat were gently transferred to a fresh polypropylene tube containing 0.7 ml of the washing buffer and centrifuged at 160 *g* for 5 minutes. The same operation was repeated once in order to pellet contaminating leukocytes and red blood cells. The supernatant was transferred to two polypropylene tubes containing 4 ml of washing buffer. After centrifugation at 2,000 *g* for 12 minutes, the platelet pellet was resuspended in resuspension buffer (137 mM NaCl, 4 mM KCL, 0.5 mM MgCl$_2$, 0.5 mM sodium phosphate, 11.1 mM dextrose, 0.1% BSA, 10 mM HEPES, pH 7.4). Platelets were fluorescently labeled with calcein AM (0.25 μg/ml; Molecular Probes Inc., Eugene, Oregon, USA) for 20 minutes at RT and infused (5×10^9 platelets/kg) through the tail vein.

In some experiments, ASA was administered in WT and *P2Y$_{12}$$^{+/-}$* mice 2 hours before FeCl$_3$-induced injury. Epinephrine (blood volume of the recipient mouse [13–17 g] estimated at 1 ml), was injected 15 minutes before injury at 1, 10, and 50 μM in WT and *P2Y$_{12}$$^{-/-}$* mice. In another experiment, 30 minutes before 50 μM epinephrine infusion, WT and *P2Y$_{12}$$^{-/-}$* mice were administered the GP IIb-IIIa inhibitor CT51464 (15) by oral gavage (50 mg/kg). Immediately after infusion of fluorescent platelets into mice of matching genotype, mice were anesthetized and mesenteric arteries (85–150 μm diameter) were studied. Vessels with a shear rate of 1,000–1,400 per second were selected using an Optical Doppler Velocimeter (Texas A&M University, System Health Science Center, Cardiovascular Research Institute, College Station, Texas, USA). Arteries were visualized using a Carl Zeiss (Oberkochen, Germany) Axiovert S100 inverted microscope (objective ×20) equipped with a 250-W HBO fluorescent lamp source (Opti Quip, Highland Mills, New York, USA) with a narrow-band FITC filter set (Chroma Technology Corp., Brattleboro, Vermont, USA) and a Hamamatsu (Tokyo, Japan) chilled CCD C5985 intensified camera connected to a VHS video recorder (Sony SVO-9500MD). One artery per mouse was filmed for 2 minutes before vessel wall injury. Vessel wall injury was generated using a modified FeCl$_3$-induced thrombosis protocol. A 2 × 1–mm filter paper was immersed into a 12.5% FeCl$_3$ solution for 2 minutes and then placed over the artery for 7 minutes. After 7 minutes, the paper was removed and the vessel covered with NaCl at 37°C. Platelet vessel wall interactions were then recorded for 33 minutes or until full occlusion occurred and lasted for more than 20 seconds.

Video analysis. Platelet vessel wall interactions and thrombus formation were analyzed in real time using Simple PCI software (Compix Inc., Imaging System, Cranberry Township, Pennsylvania, USA). In summary, the mean fluorescent intensity (which reflects the kinetics of the thrombotic process) at the site of vessel wall injury was recorded on 2 frames per second for 40 minutes and plotted automatically versus time. Each experiment was simultaneously recorded on videotape and analyzed by the computer. Hence, this software allows continuous monitoring of the thrombotic process for each animal.

Perfusion chamber experiments. The murine ex vivo perfusion chamber protocol has been described previously (16). Briefly, non-anticoagulated blood was collected from the vena cava of anesthetized mice and perfused for 2.5 minutes through either fibrinogen-coated (500 μg/ml in saline solution incubated for 2 hours at RT; Sigma-Aldrich) or human type III collagen-coated (Sigma-Aldrich) capillary chambers. Capillary chambers with a diameter of 345 μm were used to establish a shear rate of 871/s (flow rate of 212 μl/min) (17). To study binding of murine GP Ibα to human vWF (18, 19), washed platelets (3×10^8/ml supplemented with 1 mM CaCl$_2$) from WT or P2Y$_{12}$-deficient mice were incubated with 6 μg/ml botrocetin (19), with or without 10 μM epinephrine, and perfused through human vWF-coated (100 μg/ml incubated at 4°C overnight; kind gift of Zaverio Ruggeri, The Scripps Research Institute, La Jolla, California, USA) capillary chambers at 871/s for 4 minutes. For perfusion over fibrinogen and vWF, the number of platelets present in a 300 × 150–μm window was determined using Simple PCI software. For perfusion over collagen, *P2Y$_{12}$$^{-/-}$* mice were infused intravenously with 10 mg/kg ASA (Aspegic; Sanofi-Synthelabo Inc., Malvern, Pennsylvania, USA) 2 hours before blood perfusion. Epinephrine (50 μM) was injected in ASA-treated *P2Y$_{12}$$^{-/-}$* mice 10 minutes before ex vivo blood perfusion. Mean thrombus volume (micrometer cubed per micrometer squared, corresponding to the mean area of all thrombi divided by their mean

length of adhesion) was quantified on semithin cross sections and by mean gray level measurements at 5 mm from the proximal part of the capillary using Simple PCI software.

Immunohistological staining of WT and P2Y₁₂⁻/⁻ murine thrombi formed ex vivo. Rectangular capillaries (0.3 × 0.3 mm; VitroCom, Mountain Lakes, New Jersey, USA) were coated with human type III collagen and perfused with non-anticoagulated blood (collected from the vena cava) for 2.5 minutes at 220 µl/min (840/s). Immediately after, capillaries were rinsed for 15 seconds, fixed in 2% paraformaldehyde at 4°C for 1 hour, rinsed three times with PBS/0.5% BSA, then incubated for 45 minutes either with FITC-conjugated anti-mouse P-selectin (1:25 dilution; PharMingen, San Diego, California, USA) or goat anti-human Gas6 (100 µg/ml; Santa Cruz Biotechnology Inc., Santa Cruz, California, USA), followed by TRITC-conjugated rabbit anti-goat Ab (1:1,000 dilution; Jackson ImmunoResearch Laboratories Inc., West Grove, Pennsylvania, USA). In some experiments, thrombi were fixed for 30 minutes, incubated for 1 hour with 1 mg/ml Alexa 488-fibrinogen (Molecular Probes Inc.), and rinsed four times with PBS/0.5% BSA.

FACS study of the level of GP IIb-IIIa activation. Washed platelets (± 1 mM CaCl₂) from WT and P2Y₁₂⁻/⁻ mice were incubated for 1 hour at 37°C with either saline, 0.6 mM murine TRAP (SynPep Corp., Dublin, California, USA), or 5 µM ADP, in the presence or absence of 1, 10, or 50 µM epinephrine and 200 µg/ml Alexa 488-fibrinogen (Molecular Probes Inc.). Analysis of platelet-bound Alexa 488-fibrinogen was performed using a FACSort flow cytometer (Becton Dickinson Immunocytometry Systems, San Jose, California, USA).

All procedures conformed to institutional guidelines and to the Guide for the Care and Use of Laboratory Animals (The NIH, Bethesda, Maryland, USA).

Statistical analysis. Bleeding time values are expressed as mean plus or minus SEM. The effect of various concentrations of epinephrine in vivo as well as the bleeding time study were tested by one-way ANOVA and comparison analyzed using Dunnett multiple comparison tests. Statistical significance of the difference between two groups of data was tested by student *t* tests.

Results

Generation of the P2Y₁₂⁻/⁻ mice and hemostatic parameters. We generated P2Y₁₂-null mice by a gene-targeting strategy (Figure 1, a and b). Mice lacking P2Y₁₂ were viable, fertile, and produced viable offspring and normal litter sizes. Platelet counts in *P2Y₁₂⁻/⁻* mice, as well as counts for other blood cell lineages, were essentially identical to WT mice (data not shown). We compared the aggregation responses of PRPs from WT, *P2Y₁₂⁺/⁻*, and *P2Y₁₂⁻/⁻* mice using 0.5 µM and 10 µM ADP (Figure 2, a and b). As expected, lack of P2Y₁₂ dramatically affected the aggregation process induced by ADP in the *P2Y₁₂⁻/⁻* mice at both ADP concentrations, with results in the *P2Y₁₂⁺/⁻* mice more similar to WT platelets. Shape change in response to either agonist was normal in both WT and P2Y₁₂-deficient platelets, in agreement with a previous report (20). We also examined aggregation in all three genotypes using 1 and 20 µg/ml collagen (Figure 2, c and d) as well as 1 and 2.5 mM murine TRAP (Figure 2, e and f). At low doses of each of these agonists, responses in the *P2Y₁₂⁻/⁻* mice are eliminated or severely impaired relative to WT platelets, but there is essentially no difference in the aggregation response of all three geno-
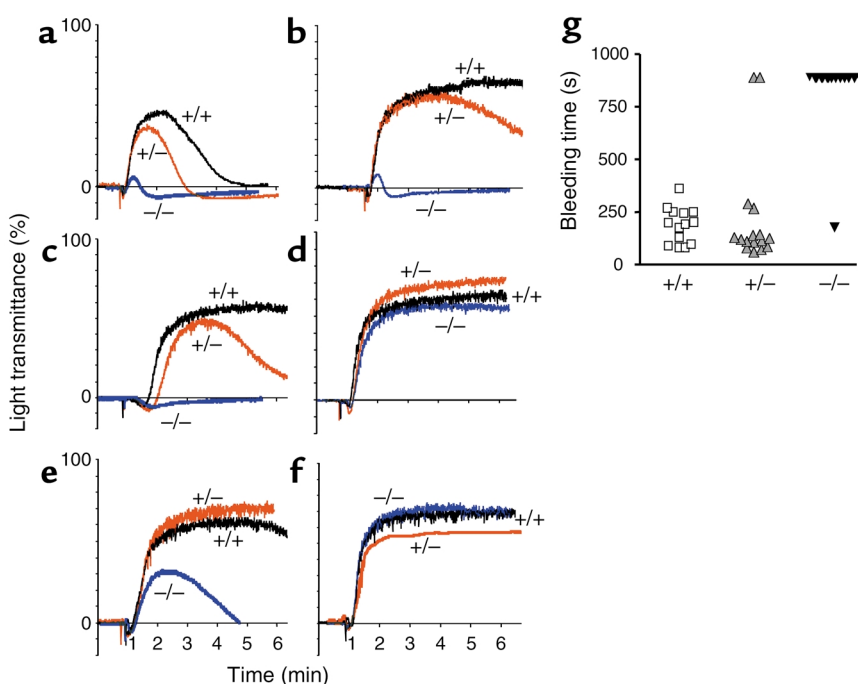

Figure 2
Aggregation measurements in PRP obtained from WT (+/+), *P2Y₁₂⁻/⁻* (–/–), or *P2Y₁₂⁺/⁻* (+/–) mice in response to (**a**) 0.5 µM ADP, (**b**) 10 µM ADP, (**c**) 1 µg/ml collagen, (**d**) 20 µg/ml collagen, (**e**) 1 mM mTRAP, and (**f**) 2.5 mM mTRAP. Traces are representative of data obtained from two independent experiments (blood from four mice pooled for each experiment). (**g**) Tail bleeding times for WT (*n* = 14), *P2Y₁₂⁺/⁻* (*n* = 18), and *P2Y₁₂⁻/⁻* mice (*n* = 15) littermates. Values are expressed as mean ± SEM. *$P < 0.01$ versus WT and *P2Y₁₂⁺/⁻* mice (using Dunnett test).
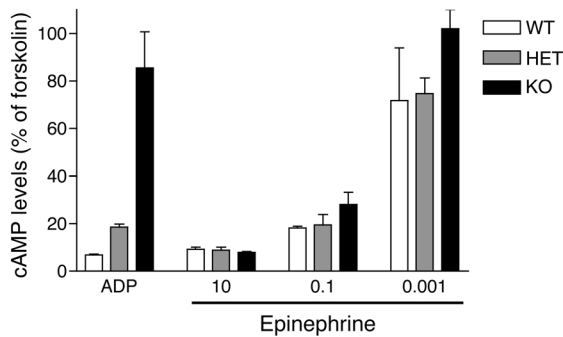
Figure 3
Inhibition of cAMP by ADP and epinephrine in WT, $P2Y_{12}^{+/-}$, and $P2Y_{12}^{-/-}$ mice. Data are expressed as the mean ± SD of triplicate measurements normalized to cAMP levels in the presence of 50 μM forskolin (100%) and are representative of two independent experiments. HET, heterozygous.

types using the higher concentration of both agonists, suggesting loss of $P2Y_{12}$ causes a shift in the dose response of both collagen and murine TRAP.

Mice deficient in $P2Y_{12}$ have a severe prolongation of the bleeding time compared with WT and $P2Y_{12}^{+/-}$ (Figure 2g). The results of the $P2Y_{12}^{+/-}$ mice are consistent with those observed in patients that are heterozygous at the $P2Y_{12}$ locus (21, 22) who also display normal bleeding times.

As $P2Y_{12}$ couples to inhibition of adenylyl cyclase through $G_{\alpha i}$, we also examined the ability of ADP to repress forskolin-stimulated cAMP levels in washed platelets from WT, $P2Y_{12}^{+/-}$, and $P2Y_{12}^{-/-}$ mice. As expected, no repression by ADP of forskolin-induced cAMP levels was observed in $P2Y_{12}$-deficient mice (Figure 3); however, the level of repression by ADP in $P2Y_{12}^{+/-}$ platelets was similar to that of WT platelets, suggesting that approximately 50% of the level of $P2Y_{12}$ receptor is sufficient to mediate inhibition of adenylyl cyclase through the $G_{\alpha i}$ pathway. Since epinephrine, which inhibits adenylyl cyclase through $G_{\alpha z}$ in mouse platelets, can compensate for blockade or lack of $P2Y_{12}$, we examined the ability of epinephrine (0.001–10 μM) to repress forskolin-stimulated cAMP levels in platelets from all three genotypes of mice. As seen in Figure 3, no impairment of cAMP repression was observed in all three genotypes over a range of epinephrine concentrations.

In vivo thrombotic profile of $P2Y_{12}^{-/-}$mice. Using real-time continuous analysis of the thrombotic process, we observed that the time for appearance of first thrombus bigger than 20 μm was significantly delayed in $P2Y_{12}^{-/-}$ ($P = 0.0063$ versus WT) and in $P2Y_{12}^{+/-}$ ($P = 0.0381$ versus WT) (Figures 4a and 5a), whereas the transient platelet interactions that immediately follow vessel wall injury (i.e., tethering and rolling) were not affected (data not shown). We found that $P2Y_{12}^{-/-}$ mice developed a cyclic thrombotic process (Figure 4a) with more than 50 thrombi of intermediate size (between 25 and 50 μm diameter)

embolizing between the 8–15 minute period in contrast to the WT and heterozygous mice where only a few (three to five) large (>50 μm) thrombi embolized before occlusion (Figure 5b). Time for occlusion was significantly increased in $P2Y_{12}^{-/-}$ mice ($P < 0.0001$) because only one out of nine animals reached occlusion after 38 minutes (Figure 5c). Interestingly, in heterozygous animals both time for appearance of first thrombus and time for occlusion were delayed compared with WT mice (Figure 5, a and c). ASA infusion (10 mg/kg) had limited efficacy in both WT and $P2Y_{12}^{+/-}$ mice (Figure 5, b and c). This dose of ASA was demonstrated to completely block arachidonic acid–induced aggregation in mouse platelets (data not shown). Epinephrine corrected the delay in time for appearance of $P2Y_{12}^{-/-}$ mice at all three concentrations used (1, 10, and 50 μM; $P < 0.001$) and accelerated (at 10 and 50 μM) the thrombotic process in $P2Y_{12}^{-/-}$ mice, but did not fully restore stability (Figure 4b and Figure 5, b and c). Although use of a GP IIb-IIIa inhibitor (CT51464) prevented occlusion in both WT and $P2Y_{12}^{-/-}$ epinephrine-treated mice, some cyclic thrombotic process still occurred in the WT/epinephrine-treated group, but not in the $P2Y_{12}^{-/-}$ mice (Figure 4b and Figure 5b).

In vitro and ex vivo profiles of $P2Y_{12}^{-/-}$ platelet deposition. Because our in vivo results indicated that the appearance of thrombi was delayed in $P2Y_{12}^{-/-}$ versus WT mice, we compared the adhesion/activation thrombus formation processes on purified proteins under high shear rate conditions in order to understand the role of $P2Y_{12}$ in these processes. vWF has a proven role in arterial thrombosis (23): indeed, $P2Y_{12}^{-/-}$ platelets adhered substantially less on vWF-coated surface, even in the absence of ASA, compared with WT
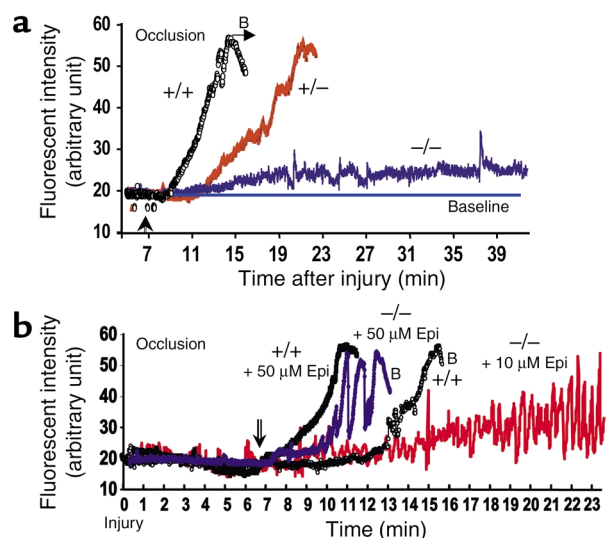

Figure 4
(**a**) In vivo arterial thrombotic profile of WT, $P2Y_{12}^{+/-}$, and $P2Y_{12}^{-/-}$ mice. (**b**) Modulation of the thrombotic profile upon epinephrine treatment. B, bleaching; Epi, epinephrine. Vertical arrows correspond to the time when filter paper was removed from the artery.
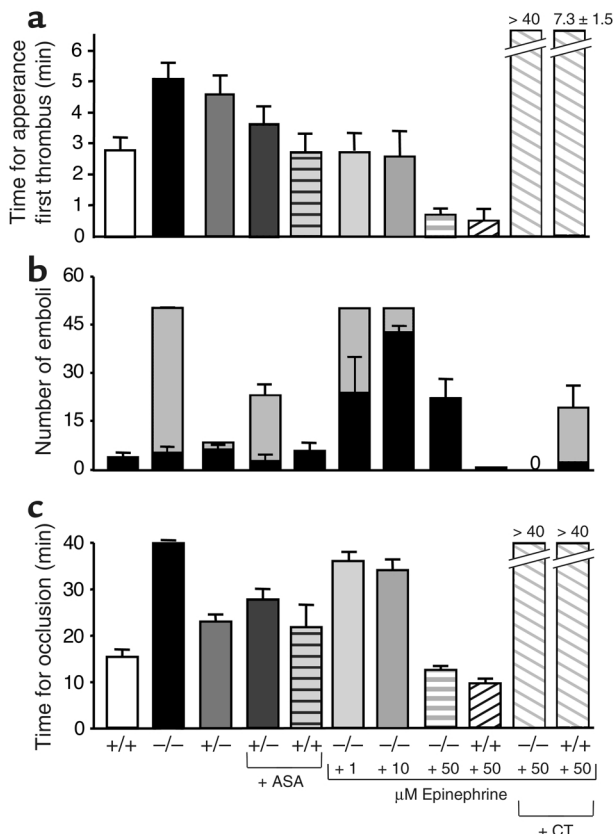
a

Time for appearance first thrombus (min)

> 40 | 7.3 ± 1.5

b

Number of emboli

c

Time for occlusion (min)

> 40 | > 40

+/+ −/− +/− +/− +/+ −/− −/− −/− +/+ −/− +/+
                    + ASA   +1 +10 +50 +50 +50 +50
                              μM Epinephrine
                                                    + CT

Figure 5

Characteristics of the in vivo thrombotic process. (**a**) A comparison of the time for appearance of first thrombus greater than 20 μm for all three *P2Y₁₂* genotypes, WT, *P2Y₁₂⁺/⁻*, and *P2Y₁₂⁻/⁻*, with and without addition of either ASA, epinephrine (1, 10, or 50 μM), or epinephrine plus CT51464 (+CT). (**b**) *P2Y₁₂⁻/⁻* thrombotic process was characterized by constant embolization of thrombi greater than 25 μm and less than 50 μm (dotted bars) between 8 and 15 minutes after injury, whereas only a few large thrombi (greater than 50 μm, black bars) embolized in both WT and *P2Y₁₂⁺/⁻* mice before occlusion of the blood vessel. Intravenous injection of epinephrine accelerated the thrombotic process but did not fully restore stability. When more than 50 thrombi embolized during the 7-minute period, a value of 50 was fixed. This explains the lack of error bars for the *P2Y₁₂⁻/⁻* groups treated with 1 and 10 μM epinephrine. (**c**) Time for occlusion of mesenteric arteries. P2Y₁₂ deficiency significantly increased (*P* < 0.0001) the time for occlusion. *P2Y₁₂⁺/⁻* mice presented an increased time for occlusion (*P* < 0.01 versus WT). ASA treatment of WT mice prolonged the time for occlusion (*P* < 0.05). Epinephrine (50 μM) restored occlusion in *P2Y₁₂⁻/⁻* mice. GP IIb-IIIa antagonism in epinephrine-treated mice prevented occlusion, but was accompanied by severe bleeding at the site of vascular surgery (*n* = 5–12 animals).
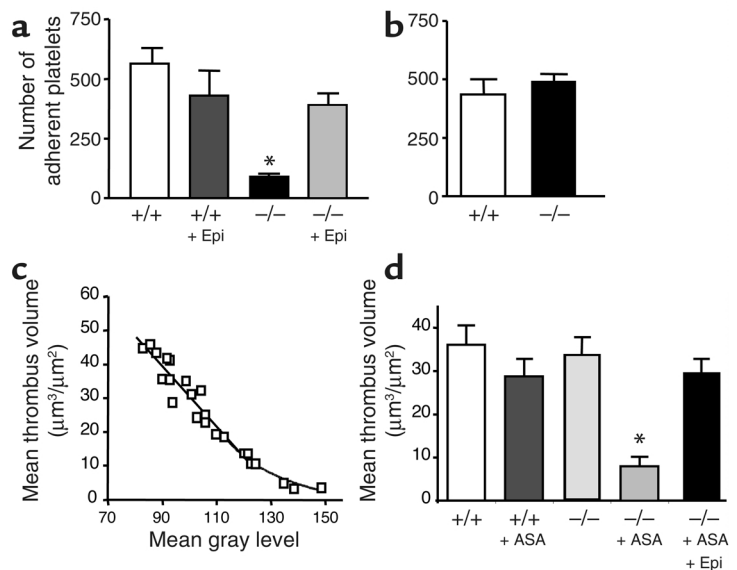
platelets (Figure 6a). This defect was fully corrected by 10 μM epinephrine, suggesting that activation of the G_i pathway was the missing signaling event. Platelet adhesion over fibrinogen was not affected by the lack of P2Y₁₂ (Figure 6b).

Ex vivo, platelet adhesion over collagen was slightly increased in the *P2Y₁₂⁻/⁻* mice (40% ± 4.5% for *P2Y₁₂⁻/⁻* versus 31.1% ± 1.5% for WT). Mean thrombus volume using whole blood from WT, *P2Y₁₂⁻/⁻*, and ASA-treated WT or *P2Y₁₂⁻/⁻* mice was obtained from

cross sections and plotted against their respective gray level measurement (Figure 6c). We confirmed that the antithrombotic activity of ASA synergized with that of *P2Y₁₂⁻/⁻* mice because ASA-treated *P2Y₁₂⁻/⁻* mice presented a profound reduction in thrombus volume (*P* < 0.001 versus WT), which was corrected upon 50 μM epinephrine infusion (Figure 6d). Because the shear rate was fixed by both the peristaltic pump and the diameter of the perfusion chamber, this excluded a possible involvement of a rheological effect of epinephrine. Although there were no significant differences in thrombus volume between *P2Y₁₂⁻/⁻* and WT thrombi, *P2Y₁₂⁻/⁻* thrombi formed over collagen were loosely packed and platelets present at the apex of the thrombi were less activated than in WT thrombi, as indicated by the

Figure 6

Perfusion chamber experiments. (**a**) Washed platelets resuspended in presence of botrocetin were perfused through a human vWF-coated capillary at 871/s for 4 minutes. (**b**) Non-anticoagulated whole blood was perfused over fibrinogen at 871/s for 2.5 minutes. No differences were observed between WT and *P2Y₁₂⁻/⁻* blood. (**c**) Twenty-five perfusion chambers were used to establish the mean gray level thrombotic profile in the 345-μm diameter capillary, including WT, *P2Y₁₂⁻/⁻*, and *P2Y₁₂⁻/⁻* mice treated with ASA. (**d**) ASA-treated or untreated non-anticoagulated blood of WT or *P2Y₁₂⁻/⁻* mice was perfused over collagen at 871/s. Epinephrine infusion (50 μM) corrects the inhibition observed with the combination P2Y₁₂ deficiency/ASA uptake (10 mg/kg). Values were expressed as the mean ± SEM of at least six animals per group.*P* < 0.001.
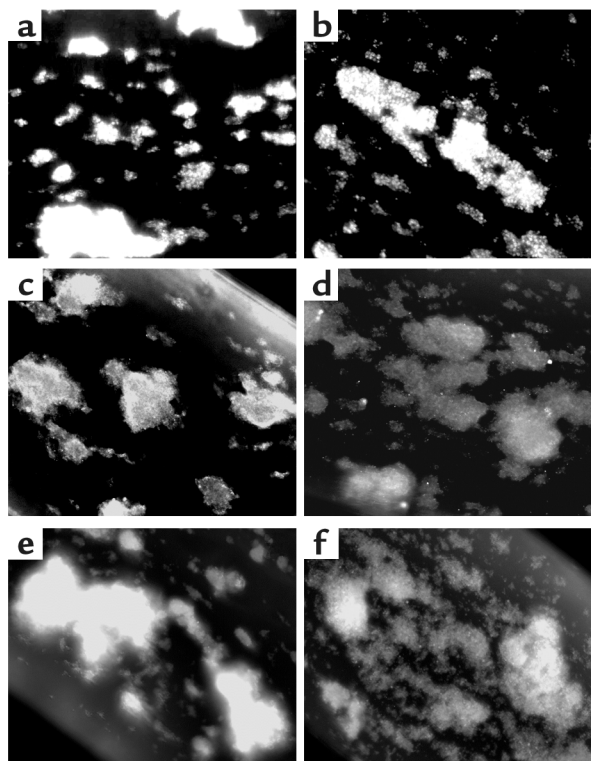
a

Number of adherent platelets

+/+ +/+ + Epi −/− −/− + Epi

b

+/+ −/−

c

Mean thrombus volume (μm³/μm²)

Mean gray level

d

Mean thrombus volume (μm³/μm²)

+/+ +/+ + ASA −/− −/− + ASA −/− + ASA + Epi

Figure 7

Level of platelet activation at the apex of arterial thrombi. Thrombi formed after a 2.5-minute perfusion period of WT (**a**, **c**, and **e**) and $P2Y_{12}^{-/-}$ (**b**, **d**, and **f**) blood at 840/s over collagen. Fixed (but not permeabilized) thrombi were stained for P-selectin (**a** and **b**), Gas6 (**c** and **d**), and with Alexa 488-fibrinogen (**e** and **f**).

staining for P-selectin, Gas6, and the decreased binding of Alexa 488-fibrinogen (Figure 7).

FACS study of the level of platelet activation induced by various agonists. $P2Y_{12}^{-/-}$ platelets activated either with murine TRAP or ADP were found to bind less fibrinogen compared with WT mice (Figure 8). Epinephrine (10 μM) induced GP IIb-IIIa activation as reported previously (24, 25) in both WT and $P2Y_{12}^{-/-}$ platelets and potentiated fibrinogen binding in WT platelets activated by ADP. Treatment with epinephrine in ADP and mTRAP-activated $P2Y_{12}^{-/-}$ platelets gave a pattern similar to that of WT platelets treated with either agonist alone. Epinephrine effects were observed at concentrations as low as 1 μM (data not shown).

Discussion

Although the combination therapy of thienopyridines/ASA represents a successful clinical strategy for the prevention of arterial thrombosis (26, 27), the actual mechanistic basis for understanding how inhibitors of $P2Y_{12}$ act in vivo has been lacking. The role previously attributed to the platelet $P2Y_{12}$ receptor has been that of sustaining aggregation and stabilization of large aggregates, based on aggregometry studies with $P2Y_{12}$ antagonists and patients with defects in this receptor. A recent study has described

the in vitro platelet phenotype of SP1999-deficient mice ($P2Y_{12}^{-/-}$ mice) but lacked evaluation of the effect of $P2Y_{12}$ deficiency on the thrombotic process (20). By using mice deficient in $P2Y_{12}$, we now demonstrate that $P2Y_{12}$ is involved, to varying degrees, in each step of arterial thrombogenesis. The overall effect of loss of $P2Y_{12}^{-/-}$ in mice translates into a delayed cyclic thrombotic process in which injured arteries are unable to occlude, even in the absence of ASA. It thus appears that the $P2Y_{12}^{-/-}$ phenotype shares the phenotypes of both $vWF^{-/-}$ (absence of occlusion) and *fibrinogen*$^{-/-}$ (unstable thrombi) mice (1).

$P2Y_{12}$ deficiency affects each step of the thrombotic process (Figure 9). First, platelet adhesion on vWF under high shear rates was decreased in $P2Y_{12}^{-/-}$ mice, which likely represents a defect in the inside-out activation of GP IIb-IIIa. Our results in mice support those previously reported by Goto et al. (12), who demonstrated that released ADP acting on $P2Y_{12}$ is important in activation of the process that leads to firm platelet adhesion on vWF. Since vWF has a proven role in platelet adhesion and platelet-platelet interactions, this likely accounts, in part, for the observed delayed thrombus formation in vivo. Second, there is an overall platelet activation defect observed on the surface of a growing thrombus in $P2Y_{12}^{-/-}$ mice, as reflected by decreased expression of P-selectin and Gas6 and decreased fibrinogen binding on collagen-coated surfaces. As platelets release thrombogenic mediators such as CD40L and Gas6 upon activation (28, 29), this could further reduce the thrombogenicity of a $P2Y_{12}^{-/-}$ growing thrombus. In addition, a defect in platelet activation/secretion
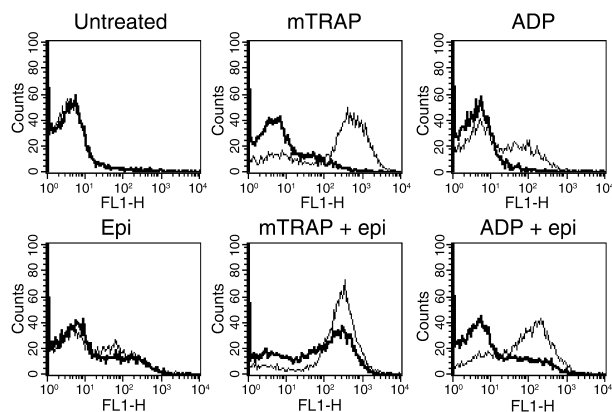

Figure 8

Flow-cytometric analysis of Alexa 488-fibrinogen binding to resting platelets, 0.6 mM mTRAP-treated platelets, and 5 μM ADP-treated platelets in the presence or absence of 10 μM epinephrine-activated (Epi) and ADP plus epinephrine–activated platelets. Thick line represents $P2Y_{12}^{-/-}$ platelets; thin line WT platelets. Epinephrine (1 and 10 μM) did not induce binding of Alexa 488-fibrinogen in absence of 1 mM $CaCl_2$ (not shown). The presence of epinephrine in ADP- and mTRAP-activated $P2Y_{12}^{-/-}$ platelets gave a pattern similar to that of WT platelets treated with the same agonist in the absence of epinephrine. Data shown are representative of at least three experiments performed in duplicate.
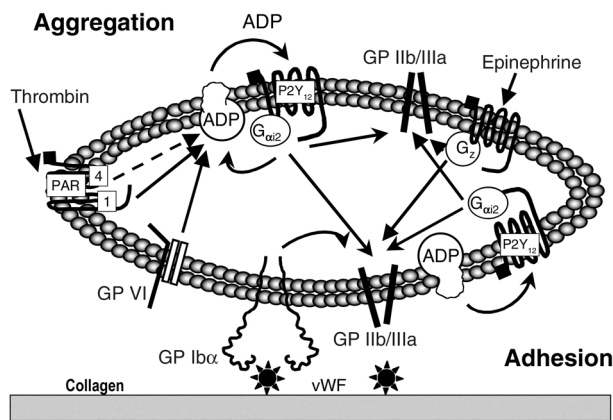
Aggregation

Figure 9

$P2Y_{12}$ at the crossroads of the arterial thrombotic process. Upon vascular injury, various thrombogenic components (i.e., collagen/vWF) are exposed to arterial blood flow. Platelet membrane GP Ibα recognizes the activated conformation of vWF, inducing various signals inside the platelets, and leads to GP IIb-IIIa activation. ADP released from platelet-dense granules participates in the firm adhesion/activation step by interaction with $P2Y_{12}$, leading to activation of GP IIb-IIIa. Simultaneously, collagen-induced platelet activation through GP VI (42) leads to GP IIb-IIIa activation, resulting in adhesion and aggregation. ADP-$P2Y_{12}$ interactions (downstream of GP Ibα signaling and subsequent stimulation of the thrombin receptor) (43) also mediate the recruitment of circulating platelets to a growing thrombus. $P2Y_{12}$ might also affect thrombus stability as a result of low surface expression of known secondary platelet agonists (P-selectin, Gas6, CD40L [see ref. 44] not shown on the scheme). PAR, protease-activated receptor.

may also result in a decreased amount of secreted vWF, a known important player of the thrombotic process (30–32). Third, activation by mTRAP and ADP was impaired in $P2Y_{12}^{-/-}$ mice. The combined consequences of these defects would be sufficient to cause a cyclic thrombotic process preventing arterial occlusion in vivo.

Because $P2Y_{12}$ and the adrenergic receptor both repress intracellular cAMP through $G_{\alpha i2}$ and G_z and are both capable of activating Rap-1, which likely plays a role in GP IIb-IIIa activation (33, 34), we investigated the physiological response of $P2Y_{12}^{-/-}$ mice challenged with epinephrine. Stimulation of the platelet adrenergic receptor α_{2a} by epinephrine corrected the overall phenotype attributed to $P2Y_{12}$ deficiency except for thrombus stability in vivo. This observation suggests that although both G_i and G_z repress cAMP, there are unique features of the $P2Y_{12}/G_i$ pathway that are critical for thrombus stability and that are not compensated by epinephrine/G_z. Because epinephrine also contributes to GP IIb-IIIa activation, however, one cannot exclude that part of the correction is due to the circulation of preactivated platelets. Our FACS study confirmed that ADP and epinephrine signal via two different pathways (7, 35, 36) and that epinephrine potentiates the effect of ADP alone, even in WT mice. Interestingly, the defect in fibrinogen binding to $P2Y_{12}^{-/-}$ platelets was more pronounced than that of $G_{\alpha i2}^{-/-}$ platelets (13).

Another major finding is that even though $P2Y_{12}^{+/-}$ mice display a significant increased time for in vivo occlusion, they have a normal bleeding time. ASA infusion in $P2Y_{12}^{+/-}$ mice failed to confer a knockout phenotype. This likely indicates that some subtle differences exist between murine and human $P2Y_{12}$ activities because antithrombotic activity of ASA only partially modulated the $P2Y_{12}^{+/-}$ phenotype in vivo, whereas it is known that ASA synergizes $P2Y_{12}$ antagonism in humans. Overall, our in vitro, ex vivo, and in vivo results using $P2Y_{12}^{-/-}$ mice agree well with studies in humans using $P2Y_{12}$ antagonists, because mouse platelets behave similarly to human platelets in response to ADP (20), except for lack of dense-granule release in mouse platelets compared with humans (37).

The current thienopyridine $P2Y_{12}$ antagonists (clopidogrel and ticlopidine) require hepatic metabolism in order to block $P2Y_{12}$, and recent studies have demonstrated that even a bolus dose in combination with ASA requires at least 6 hours to reach maximal antithrombotic activity (38, 39). Furthermore, Gurbel et al. demonstrated that the normal dosing regimen of clopidogrel results in less than 40% blockade of ADP-induced aggregation and is highly variable between individuals (4). It is therefore conceivable that direct-acting $P2Y_{12}$ inhibitors with improved pharmacokinetic properties may achieve better efficacy if they target greater than 50% inhibition, as our in vivo results suggest.

The present study also highlights two main issues in regard to predicted therapeutic efficacy of $P2Y_{12}$ antagonists. First, we have found that total $P2Y_{12}$ deficiency dramatically affects the in vivo thrombotic process and ex vivo thrombosis on surfaces expressing vWF and collagen, both known components of atherosclerotic plaques. The data predict, therefore, that more efficient inhibition of $P2Y_{12}$ than is afforded by the currently available antagonists would be more efficacious, even though it is recognized that $P2Y_{12}$ antagonism does not inhibit thrombosis over tissue factor, a third highly thrombogenic constituent of an atherosclerotic plaque (40). Second, higher concentrations of $P2Y_{12}$ antagonists or combined strategies of $P2Y_{12}$ antagonism coupled either to GP IIb-IIIa inhibitors (as observed on Figure 5c) or direct thrombin inhibitors could represent an alternative strategy for the subpopulation of patients (10–30%) who don't respond to ASA (41).

Acknowledgments

1. Ni, H., et al. 2000. Persistence of platelet thrombus formation in arterioles of mice lacking both von Willebrand factor and fibrinogen. *J. Clin. Invest.* **106**:385–392.

2. Hollopeter, G., et al. 2001. Identification of the platelet ADP receptor targeted by antithrombotic drugs. *Nature.* **409**:202–207.

3. Gachet, C. 2001. ADP receptors of platelets and their inhibition. *Thromb. Haemost.* **86**:222–232.

4. Gurbel, P.A., Malinin, A.I., Callahan, K.P., Serebruany, V.L., and O'Connor, C.M. 2002. Effect of loading with clopidogrel at the time of coronary stenting on platelet aggregation and glycoprotein IIb/IIIa expression and platelet-leukocyte aggregate formation. *Am. J. Cardiol.* **90**:312–315.

5. CAPRIE Steering Committee. 1996. A randomised, blinded, trial of clopidogrel versus aspirin in patients at risk of ischaemic events (CAPRIE). CAPRIE Steering Committee. *Lancet.* **348**:1329–1339.

6. The CURE Trial Investigators. 2001. Effects of clopidogrel in addition to aspirin in patients with acute coronary syndromes without ST-segment elevation. *N. Eng. J. Med.* **345**:494–502.

7. Cattaneo, M., et al. 1990. Released adenosine diphosphate stabilizes thrombin-induced human platelet aggregates. *Blood.* **75**:1081–1086.

8. Gachet, C., et al. 1997. Activation of ADP receptors and platelet function. *Thromb. Haemost.* **78**:271–275.

9. Gayle, III, R.B., et al. 1998. Inhibition of platelet function by recombinant soluble ecto-ADPase/CD39. *J. Clin. Invest.* **101**:1851–1859.

10. Pinsky, D.J., et al. 2002. Elucidation of the thromboregulatory role of CD39/ectoapyrase in the ischemic brain. *J. Clin. Invest.* **109**:1031–1040. doi:10.1172/JCI200210649.

11. Nieswandt, B., et al. 2001. Evidence for cross-talk between glycoprotein VI and G_i-coupled receptors during collagen-induced platelet aggregation. *Blood.* **97**:3829–3835.

12. Goto, S., Tamura, N., and Handa, S. 2002. Effects of adenosine 5′-diphosphate (ADP) receptor blockade on platelet aggregation under flow. *Blood.* **99**:4644–4645.

13. Jantzen, H.M., Milstone, D.S., Gousset, L., Conley, P.B., and Mortensen, R.M. 2001. Impaired activation of murine platelets lacking $G\alpha_{i2}$. *J. Clin. Invest.* **108**:477–483. doi:10.1172/JCI200112818.

14. André, P., et al. 2000. Platelets adhere to and translocate on von Willebrand factor presented by endothelium in stimulated veins. *Blood.* **96**:3322–3328.

15. Mehrotra, M.M., et al. 2002. Spirocyclic nonpeptide glycoprotein IIb-IIIa antagonists. Part 3: synthesis and SAR of potent and specific 2,8-diazaspiro[4,5]decanes. *Bioorg. Med. Chem. Lett.* **12**:1103–1107.

16. André, P., Hartwell, D., Hrachovinova, I., Saffaripour, S., and Wagner, D.D. 2000. Pro-coagulant state resulting from high levels of soluble P-selectin in blood. *Proc. Natl. Acad. Sci. U. S. A.* **97**:13835–13840.

17. André, P., et al. 1996. Optimal antagonism of GPIIb/IIIa favors platelet adhesion by inhibiting thrombus growth. An ex vivo capillary perfusion chamber study in the guinea pig. *Arterioscler. Thromb. Vasc. Biol.* **16**:56–63.

18. Ware, J., Russell, S., and Ruggeri, Z.M. 1997. Cloning of the murine platelet glycoprotein Ibα gene highlighting species-specific platelet adhesion. *Blood Cells Mol. Dis.* **23**:292–301.

19. Wu, Y., et al. 2001. Role of Fc receptor gamma-chain in platelet glycoprotein Ib-mediated signaling. *Blood.* **97**:3836–3845.

20. Foster, C.J., et al. 2001. Molecular identification and characterization of the platelet ADP receptor targeted by thienopyridine antithrombotic drugs. *J. Clin. Invest.* **107**:1591–1598.

21. Nurden, P., et al. 1995. An inherited bleeding disorder linked to a defective interaction between ADP and its receptor on platelets. Its influence on glycoprotein IIb-IIIa complex function. *J. Clin. Invest.* **95**:1612–1622.

22. Cattaneo, M., Lecchi, A., Lombardi, R., Gachet, C., and Zighetti, M.L. 2000. Platelets from a patient heterozygous for the defect of $P2_{CYC}$ receptors for ADP have a secretion defect despite normal thromboxane A2 production and normal granule stores: further evidence that some cases of platelet "primary secretion defect" are heterozygous for a defect of $P2_{CYC}$ receptors. *Arterioscler. Thromb. Vasc. Biol.* **20**:E101–E106.

23. Ni, H., et al. 2001. Increased thrombogenesis and embolus formation in mice lacking glycoprotein V. *Blood.* **98**:368–373.

24. Shattil, S.J., Budzynski, A., and Scrutton, M.C. 1989. Epinephrine induces platelet fibrinogen receptor expression, fibrinogen binding, and aggregation in whole blood in the absence of other excitatory agonists. *Blood.* **73**:150–158.

25. Keularts, I.M., van Gorp, R.M., Feijge, M.A., Vuist, W.M., and Heemskerk, J.W. 2000. Alpha(2A)-adrenergic receptor stimulation potentiates calcium release in platelets by modulating cAMP levels. *J. Biol. Chem.* **275**:1763–1772.

26. Quinn, M.J., and Fitzgerald, D.J. 1999. Ticlopidine and clopidogrel. *Circulation.* **100**:1667–1672.

27. Mehta, S.R., et al. 2001. Effects of pretreatment with clopidogrel and aspirin followed by long-term therapy in patients undergoing percutaneous coronary intervention: the PCI-CURE study. *Lancet.* **358**:527–533.

28. André, P., et al. 2002. CD40L stabilizes arterial thrombi by a beta3 integrin-dependent mechanism. *Nat. Med.* **8**:247–252.

29. Angelillo-Scherrer, A., et al. 2001. Deficiency or inhibition of Gas6 causes platelet dysfunction and protects mice against thrombosis. *Nat. Med.* **7**:215–221.

30. Fressinaud, E., Baruch, D., Rothschild, C., Baumgartner, H.R., and Meyer, D. 1987. Platelet von Willebrand factor: evidence for its involvement in platelet adhesion to collagen. *Blood.* **70**:1214–1217.

31. André, P., et al. 1998. Role of plasma and platelet von Willebrand factor in arterial thrombogenesis and hemostasis in the pig. *Exp. Hematol.* **26**:620–626.

32. Kulkarni, S., et al. 2000. A revised model of platelet aggregation. *J. Clin. Invest.* **105**:783–791.

33. Woulfe, D., Jiang, H., Mortensen, R., Yang, J., and Brass, L.F. 2002. Activation of Rap1B by G_i family members in platelets. *J. Biol. Chem.* **277**:23382–23390.

34. Larson, M.K., et al. 2003. Identification of $P2Y_{12}$-dependent and independent mechanisms of glycoprotein VI-mediated Rap1 activation in platelets. *Blood.* **101**:1409–1416.

35. Ohlmann, P., et al. 2000. ADP induces partial platelet aggregation without shape change and potentiates collagen-induced aggregation in the absence of $G_{\alpha q}$. *Blood.* **96**:2134–2139.

36. Yang, J., et al. 2000. Loss of signaling through the G protein, G_z, results in abnormal platelet activation and altered responses to psychoactive drugs. *Proc. Natl. Acad. Sci. U. S. A.* **97**:9984–9989.

37. Rosenblum, W.I., Nelson, G.H., Cockrell, C.S., and Ellis, E.F. 1983. Some properties of mouse platelets. *Thromb. Res.* **30**:347–355.

38. Cadroy, Y., et al. 2000. Early potent antithrombotic effect with combined aspirin and a loading dose of clopidogrel on experimental arterial thrombogenesis in humans. *Circulation.* **101**:2823–2828.

39. Steinhubl, S.R., et al. 2002. Early and sustained dual oral antiplatelet therapy following percutaneous coronary intervention. *JAMA.* **288**:2411–2420.

40. Bossavy, J.P., et al. 1998. A double-blind randomized comparison of combined aspirin and ticlopidine therapy versus aspirin or ticlopidine alone on experimental arterial thrombogenesis in humans. *Blood.* **92**:1518–1525.

41. Gum, P.A., Kottke-Marchant, K., Welsh, P.A., White, J., and Topol, E.J. 2003. A prospective, blinded determination of the natural history of aspirin resistance among stable patients with cardiovascular disease. *J. Am. Coll. Cardiol.* **41**:961–965.

42. Quinton, T.M., Ozdener, F., Dangelmaier, C., Daniel, J.L., and Kunapuli, S.P. 2002. Glycoprotein VI-mediated platelet fibrinogen receptor activation occurs through calcium-sensitive and PKC-sensitive pathways without a requirement for secreted ADP. *Blood.* **99**:3228–3234.

43. Kim, S., et al. 2002. Protease-activated receptors 1 and 4 do not stimulate G_i signaling pathways in the absence of secreted ADP and cause human platelet aggregation independently of G_i signaling. *Blood.* **99**:3629–3636.

44. Hermann, A., Rauch, B.H., Braun, M., Schror, K., and Weber, A.A. 2001. Platelet CD40 ligand (CD40L) — subcellular localization, regulation of expression, and inhibition by clopidogrel. *Platelets.* **12**:74–82.